ISSN 2321-807X
Volume 13 Number4
Journal of Advances in chemistry

Computational and Experimental Investigations on Aerodynamic Characteristics of a Hatchback model Car Using Base Bleed

K Selvakumar[1], Dr.K.M.Parammasivam[2]
1 Research Scholar, Department of Aerospace Engineering, MIT campus, Anna University, Chennai, India.
kselvakumar@mitindia.edu
2 Professor, Department of Aerospace Engineering, MIT campus, Anna University, Chennai, India.
mparams@mitindia.edu

ABSTRACT

Computational and experimental tests have been conducted on a realistic passenger scale model car, to investigate drag reduction opportunities from injecting low velocity air into the base region. Various techniques to reduce the aerodynamic drag of bluff bodies through the mechanism of base pressure recovery have been investigated. The investigation is conducted in free stream and in ground proximity. It is shown that, with a base bleed hose, the overall body drag is reduced. The paper shows the method used in creating the scaled model of the car and conducting the analysis, and presents the findings to date. The paper shows that the reduction in drag increases as the mass flow rate of air is increased when the flow is deflected at the outlet. By controlling the turbulent wake to the rear of the vehicle It has been shown that base bleed can significantly decrease drag when applied to the geometry of a real hatch back model car, For the geometry studied, a bleed outlet applied to the lower portion is most effective in reducing drag. Thus the reduction in drag improves the fuel economy. The paper also discusses the feasibility of base bleed being applied to a production vehicle. Finally, both experiment and simulation suggest that the drag reduction device strongly influence the underbody flow. The device causes the mean streamlines close to the ground to turn upward more rapidly, and increase the flow velocity in this region. In summary, based on our measurements and the CFD simulations the mean pressure results show a significant increase in the base pressure when the drag reduction device is in place. The results show a reduction of the turbulence intensity as well as a rapid upward deflection of the underbody flow due to the add-on device compared to the baseline configuration. Finally the reduction of drag implies the fuel economy will be reuced.

Indexing terms/Keywords

Aerodynamics, Drag, Hatchback model car, Base bleed, CFD, Base Bleed, Reynolds Number, Fuel efficiency, Flow measurement.

Academic Discipline And Sub-Disciplines

Faculty of Mechanical Engineering / Aerospace Angineering.

SUBJECT CLASSIFICATION

Vehicle Aerodynamics.

TYPE (METHOD/APPROACH)

CFD Analysis and Wind Tunnal Expriment with scaled model of car.

1. INTRODUCTION

The influence of aerodynamics on the demand-supply relationship is through the drag force, which affects the propulsive part of the demand side. Commercial aircraft, trains, ships, and highway trucks typically operate at a relatively constant cruising speed. In typical automobile driving, however, vehicle speed varies with time or distance. An analysis of the factors affecting automobile fuel economy can best be made if the driving pattern is prescribed. (W H Hucho 1993). At any instant, the tractive force required at the tire/road interface of a car's driving wheels is (Sovran & Bohn 1981)

$$F_{TR} = \underbrace{R+D}_{\text{Road Load}} + \underbrace{M\frac{dV}{dt}}_{\text{Inertia}} + \underbrace{Mg\sin\theta}_{\text{Grade}},$$

Where FTR is the tractive force, R is the tyre rolling resistance, D is the aerodynamic drag, M is the vehicle mass g the acceleration of gravity and θ is the inclination of the angle of the road. The corresponding tractive power is

$$PTR = FTR\ V$$

and the tractive energy required for propulsion during any given driving period is

$$ETR = \int_0^T PTR\ dt.$$

for positive values of the integrand. The main reason that fuel is consumed in an automobile is to provide this tractive energy. Writing an equation for instantaneous fuel consumption, integrating it over a total driving duration, and using the mean-value theorem to introduce appropriate averages for some of the integrands, the following fundamental equation for the average fuel-consumed-per-unit-distance traveled ĝ can be obtained (Sovran 1983).

$$\bar{g} = \frac{k}{\eta_b \eta_d S} \underbrace{[E_{TR} + E_{ACC}]}_{\text{propulsion } (P_{TR} > 0)} + \underbrace{g_u}_{\text{braking and idle } (P_{TR} \le 0)},$$

where k is a fuel-dependent constant, ηb is the average engine efficiency during propulsion, ηd is the average drive train efficiency, S is the total distance traveled, EAcc is the energy required by vehicle accessories, and gu is the fuel consumption during idling and braking. The impact of drag on total vehicle fuel consumption therefore depends on the relative magnitudes of these contributions.

In general, this coefficient is vehicle as well as driving-schedule dependent (Sovran 1983), but for the midsize car being considered they are ≈ 0.14 and ≈0.46 for Urban and Highway, respectively. For the Euro mix cycle, a typical influence coefficient for cars powered by spark-ignition engines is ≈0.3, while for diesel engines it is ≈0.4 (Emmelmann 1987b). In all cases, these values presume that the drive train gearing is rematches so that the road load power-requirement curve runs through the engine's brake-specific-fuel-consumption map in the same manner at the lower drag as at the higher drag. If no other changes are made in a vehicle, the benefits of reduced drag are actually threefold: reduced fuel consumption, increased acceleration capability, and increased top speed. When maximum fuel-economy benefit is the objective the increased acceleration and top-speed capabilities can be converted to additional reductions in fuel consumption.

Conversion of the increased acceleration capability is accomplished by re gearing the drive train, as discussed above. Conversion of the increased top speed requires a reduction in installed engine power, and a corresponding percentage reduction in vehicle mass so that the acceleration capability of the vehicle is not diminis hed. The preceding discussions have presumed the absence of ambient wind while driving. In the presence of wind a vehicle's wind speed is generally different than its ground speed, and its yaw angle is generallynot zero. This affects the operating drag fo rce, and therefore vehicle fuel economy (Sovran 1984). On the average, the result is a reduction in fuel economy.

Pressure drag due to flow separation constitutes more than 90% of the total drag of bluff bodies [Aachenbach E.; 1972]. A considerable proportion of the drag of a 4x4, (that is not so prevalent in saloon cars, for example) is base drag. Base drag, a form of pressure drag, is caused as a low pressure region develops to the rear of the vehicle (the base region). This low pressure is caused by turbulence as the flow separates at the rear edges of the upper, lower and side surfaces of the car.Another form of drag to be overcome is lift induced drag. It has been suggested that in the case of road vehicles, it is not possible to define an induced drag and therefore the term 'vortex drag' is preferred [R. T. Jones 1978].

COMPUTATIONAL FLUID DYNAMICS AND EXPERIMENTAL INVESTIGATIONS

2.1 Methodology and Experimental Set up

Base bleed

Base bleed can be defined as the reduction of drag via the introduction of air or some other gas to the rearward low pressure region. Drag reduction can be achieved through repressurisation of the base region, or the air or gas may be used to control the turbulent wake of the vehicle or the trailing vortices that cause drag. Although this may still result in re pressurisation within the base region, repressurisation may not be the primary influence on the change in drag.[Lamond, Andrew et. al 2009]. However, consideration was given to bleed air being obtained thro ugh ducting from a high pressure region on the vehicle as this may be a more practical approach to a real system. The point at which air is expelled into the base region will be known as the 'bleed outlet', positioned on the rear surface of the vehicle.

2.2 CFD Testing of Scaled model

First, steady state Reynolds Averaged Navier-Stokes (RANS) equations were solved to investigate the general features of the wake flow fields for both models (without base bleed and with base bleed). insight of the flow unstea diness. Steady State CFD - Steady CFD simulations were conducted using GMTEC [21,22], a GM proprietary general purpose three-dimensional Navier-Stokes CFD code with its own pre-processor for grid generation and post-processor. In these calculations, the conditions for the CFD simulations were chosen to be the same as those expected for the wind tunnel tests.

This involved the use of an inlet condition, where a uniform inlet velocity of 52 m/s was assumed. The tunnel exit was modeled using outflow condition and no slip conditions were employed at the test-section floor and walls. The RNG k-e turbulence model was used and the near-wall flow was computed using wall functions. Due to the geometric symmetry conditions of the model, only half the model was simulated. A total of 146126 tetrahedral elements with a minimum mesh size of 2 mm were used in this study. The solutions were carried out on a SGI Origin computer with one processor and typically convergence of the solution required about 1200 iterations and a bout 490,000 seconds CPU-time. Transient CFD - In this approach both configurations (SB and MSB) were simulated using the Fluent CFD code with the V2F turbulence model [23].

2.2.1 Method Involving Of Drag Reduction Using Base Bleed

Designers have come up with all sorts of tricks to lower drag, from reducing a car's frontal area to molding in small

winglets under the trunk area to diffuse the air that comes out from underneath it. But drag is just one aerodynamic factor that's at work on car. Two other forces we have probably heard about before are lift and down force. Look at the side view of a modern car and the shape looks something like the cross-section of an airplane wing, there could be enough lift to unload the tires and suspension, which will affect the car's traction and handling. To investigate the aerodynamic performance of a car,computational analysis have been carried out using

2.2.2 CFX and ICEM CFD software

After the mesh was done “check mesh” option was run to check for any uniformity problems The detected problems were suitably solved. A quality check was done for the mesh in which the minimum quality was set to about 0.51. The output postprocessor was selected to be ANSYS CFX and it was saved in .cfx5 format.

2.2.3 Dimension sheet of car

Specification	Length in mm
Overall length	3620
Overall width	1475
Overall height	1460
Ground clearance	160
Wheelbase	2360
Front tread	1295
Rear tread	1290

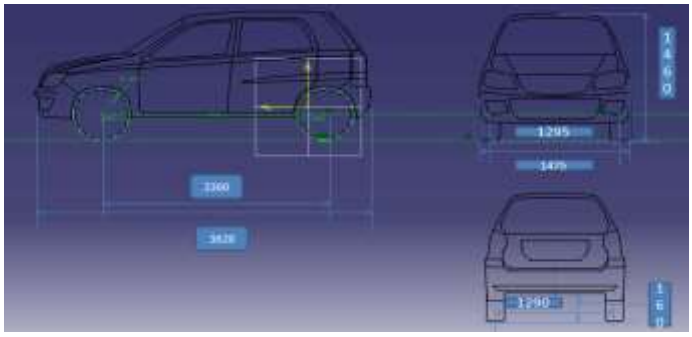

Fig.1 CATIA Designed Scaled model car

2.3 Experimental Testing of Scaled Model

The experimental study was conducted in a subsonic closed-loop suction type wind tunnel located in the Aerospace Engineering Department of MIT Anna University Chennai. The tunnel has a test section of 3x4 ft (0.9144 m x 1.2192 m) in cross section with optically transparent walls. The wind tunnel has a contraction section upstream of the test section with a set of honeycombs, screen structures, and a cooling system installed ahead of the contraction section to provide uniform low turbulent airflow into the test section. Based on the integration of the measured surface pressure distributions around the test model, the resultant wind loads (i.e., the lift and drag forces) acting on the test model can be determined by neglecting the small friction force acting on the test model.

The nose features a single opening for the front grille and side air intakes, with aerodynamic sections and profiles designed to direct air to the coolant radiators and the new flat underbody. The nose also sports small aero elastic winglets which generate down force and, as speed rises, deform to reduce the section of the radiator intake and cut drag.Technical development of the car’s shaped started using CFD (Computational Fluid-Dynamic) techniques which helped optimize the different cross section of base bleed and interaction of the internal flows prior to wind tunnel testing.

Fig.2 Subsonic closed-loop wind tunnel

Fig.3 Scaled model car in the wind tunnel

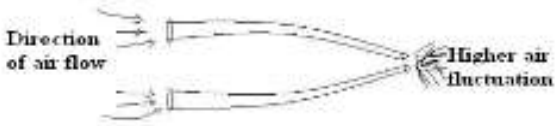

Fig 4. Location of base bleed in car and attachment Fig 5 Scaled model car in the wind tunnel Base Bleed

Table:1 Comparison of Drag Force Cd and Reynolds Number (CFD Results)

Velocity (m/s)	Drag Coefficient (C_d)		Drag Force (N)		Reynolds number
	Without Base Bleed	With Base Bleed	Without Base Bleed	With Base Bleed	
4	WO Bleed	With Bleed	9.99221	9.93891	957707.54
8	0.45	0.41	41.2282	38.4152	191415.07
12	0.31	0.27	94.0676	88.8164	287122.61
16	0.25	0.21	170.988	158.818	382830.15
20	0.23	0.2	267.893	247.874	478537.69

Table:2 Comparison of Drag Force Cd and Reynolds Number (Experimental Results**)**

Velocity (m/s)	Drag Coefficient (C_d)		Drag Force (N)		Reynolds number
	Without Base Bleed	With Base Bleed	Without Base Bleed	With Base Bleed	
4	0.65	0.62	9.13221	8.73891	1057707.54
8	0.47	0.44	35.2282	32.4672	295415.07
12	0.42	0.38	82.0676	75.9242	387122.61
16	0.37	0.34	148.568	134.535	452830.15
20	0.35	0.31	235.358	207.578	576577.69

3. MEASUREMENT RESULTS AND DISCUSSIONS

The following graph shows the comparison of pressure distribution on passenger car model with and without base bleed attachment.

3.1 Pressure Contour from CFD at 20m/s

Simulations were run at 5 speeds (4m/s ,8m/s ,12m/s ,16m/s and 20m/s)for both the without the base bleed and with base bleed. The focus of this paper is to show how to obtain a CFD simulation from a complicated CAD model and steps that can be taken to efficiently accomplish that process. The simulation results are simply presented here as an example of what can be learned from a CFD simulation. Without and with base bleed attachment of the entire car. Figure 6 shows the down force (negative lift) and drag values for each simulation.

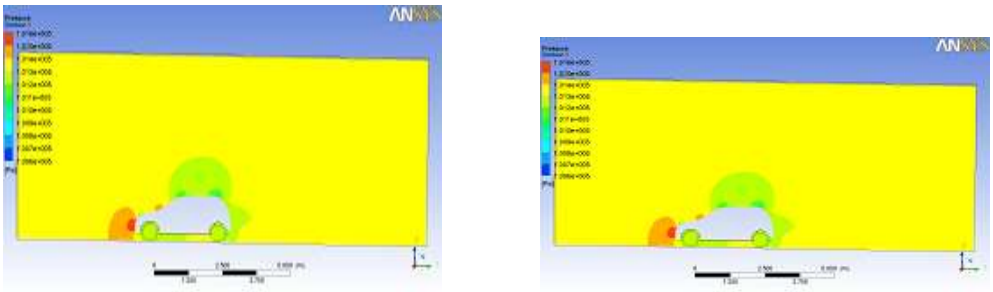

Fig.6 Pressure distribution in longitudinal axis without and with Base bleed CFD (ar 20m/s)

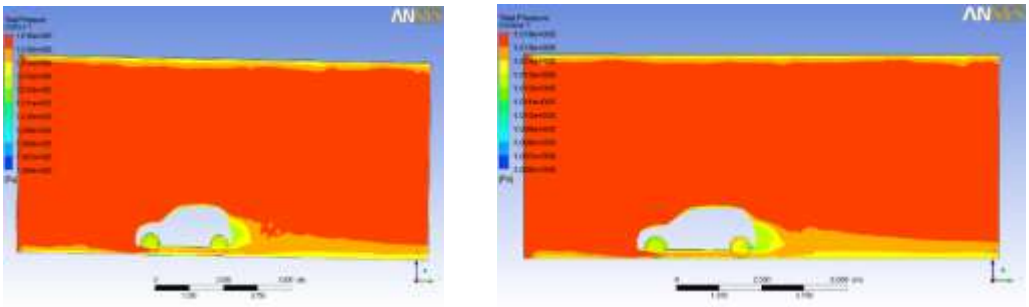

Fig.7 Total Pressure distribution in longitudinal axis without and with Base bleed CFD (ar 20m/s)

The prediction of the pressure distribution on the roof, Fig. 6, is overall accurate as well as mesh-independent. In agreement with observations in [Perzon and Davidson (2000)], very small differences to the experiments are found close to the trailing edge. The boundary layer growth in this region affects the base pressure at the upper rear end of the vehicle. Furthermore, the steady-state calculation deviates slightly from the transient analyses, which are conform on the entire roof. As with the roof pressure, the pressure distribution over the front surface of the car is overall predi cted satisfactorily, see Fig.7. However, the pressure near the stagnation point differs from the experimental data. This inaccurate behaviour in this region has also been observed in [Perzon and Davidson (2000)]. The main difference is to be found due to the boundary layer meshing type, see Fig. .6b. Contra-intuitively, the stagnation pressure is over predicted for all analyses utilizing a constant element growth rate from the boundary layer through the adjacent cell layers. The grids with abrupt coarsening off of the boundary layer approximate the stagnation pressure more accurate. Nevertheless, the clear deviations from the experimental data are independent from the core resolution and first layer height. The pressure loss at the upper rear end. However, it cannot reproduce the slight pressure rise in the lower part, which is described by the experimental data and approximated by the medium grid. The steady state simulation over predicts the pressure along the whole base, in accordance to [Perzon and Davidson (2000)].

3.2 Velocity Contour from CFD (ar 20m/s)

The reason for the expanding of velocity streamlines in the case of geometry without base bleed is that the air after passing over the rear windshield travels directly to the ground. That air has a higher speed and comes into collision behind the car with the air from below the car which has a lower speed. So the expanding of velocity streamlines are caused by distancing from the car. By using the base bleed , the opposite occurs, because the airflow is directing down wards through the elliptical hole on the front bottom by the base bleed attachment and thus allows slower air from below the car to free flow by distancing from the car, so there is no expanding of the airflow, Figure 8

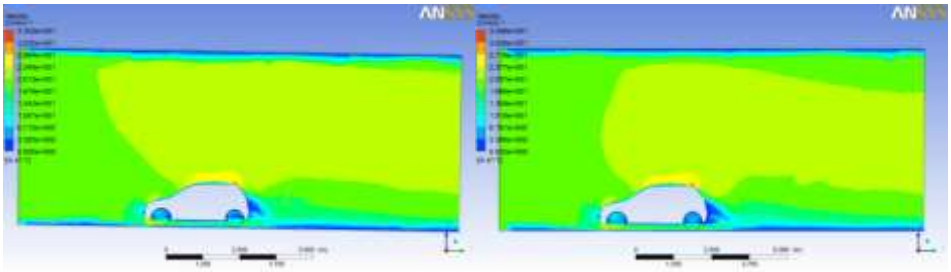

Fig.8 Velocity contour in longitudinal axis without and with Base bleed CFD (ar 20m/s)

3.3. Pressure distribution study without Base-Bleed attachment (Experimental work)

Fig.9 shows representation of pressure distribution trend, from the above graph it is clearly visible, at different range of velocities (4m/s, 8m/s, 12m/s, 16m/s, 20m/s) pressure on front bumper (Stagnation point) area is very high such as nearly -0.1 N/mm2 (except 4m/s due to low stream). From the bumper pressure reduces towards bonnet nose area. Then again increasing slowly in front hood, pressure will again get peak at the meeting point of front hood and windscreen. Then pressure will drastically drops to lowest point at the starting point of roof. From this graph it is clearly visible that there is a negative pressure difference between the frontal area and rear area of the car model. Due to this the drag force will be more in this car model without base-bleed attachment. The flow arrives at a velocity of 5 m/s at the vehicle and as it turns around the leading edges of its front face, it accelerates up to a maximum of 6.7 m/s along the sides. Due to the discontinuity in the curvature of the junction between the rounded leading edge and the flat side face of the vehicle, the boundary layer separates and forms a small separation bubble.

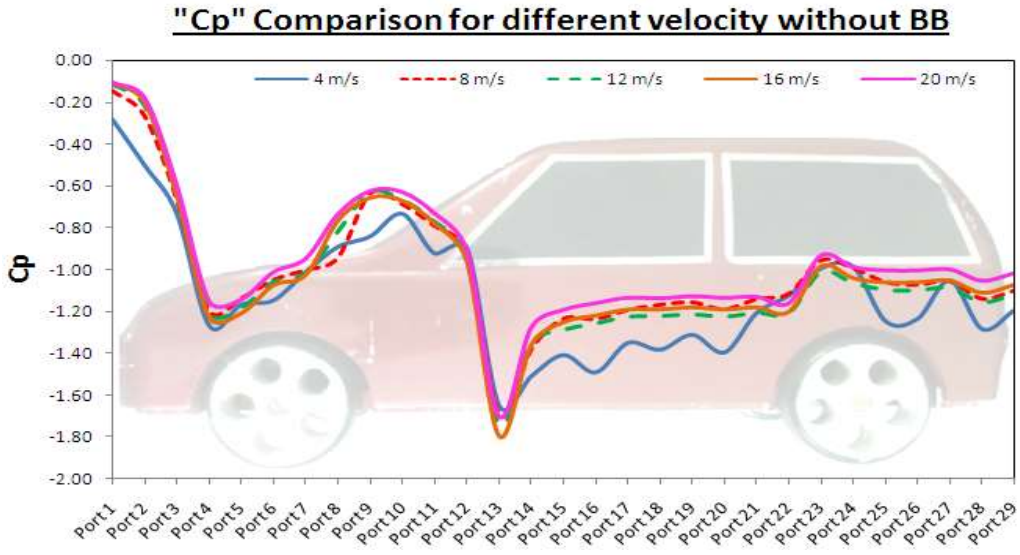

Fig.9 Pressure distribution curve without Base-Bleed attachment

Fig.10 represents the graphical representation of pressure distribution with base-bleed attachment. Here, pressure on bumper reduced by 20% and pressure has been increased by 6% at rear side of the car. Even at the higher velocities (12m/s, 16m/s, 20m/s) pressure at rear side increased considerably. Due to this pressure variation between frontal area and rear side of the car model will reduced considerably. From the stagnation point at the front of the vehicle, the pressure drops swiftly as the flow accelerates over the radiator grill and gains steadily over the bonnet of the car. As the flow is backed up at the junction between bonnet and windshield, the pressure coefficient reaches a local maximum after which the pressure decreases again over the windshield.

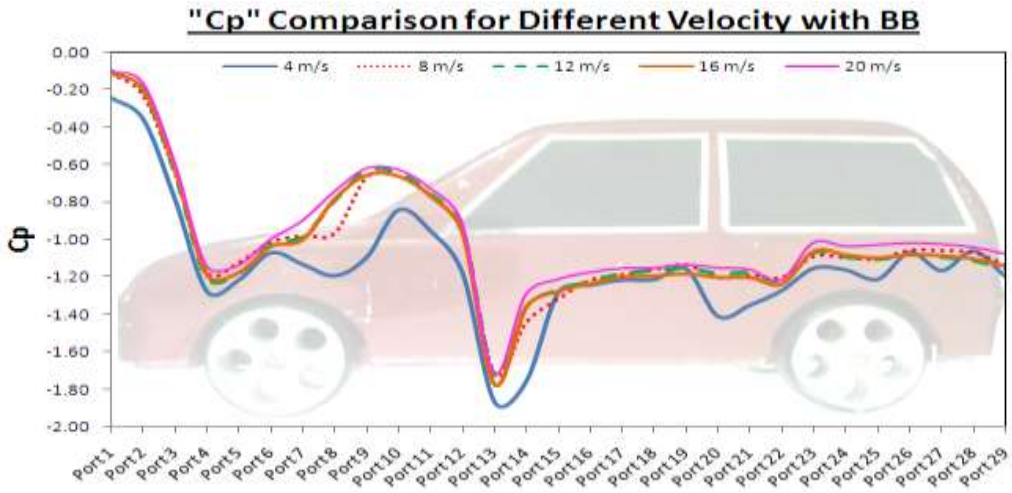

Fig. 10 Pressure distribution curve with Base-Bleed attachment

3.4. Drag force Comparison

It is clearly evident from the (Fig.11) that the value of drag force decreases due to the addition of base-bleed setup. This can be attributed due to the escaping of air flow with the help of base-bleed attachment. For varying velocities Fd will be considerably lesser compared to without base bleed attachment. Even in high velocity also the drag co-efficient will be lesser compared to without base-bleed attachment. Hence, it is observed that base-bleed attachment will be useful at lower velocity to reduce drag force.

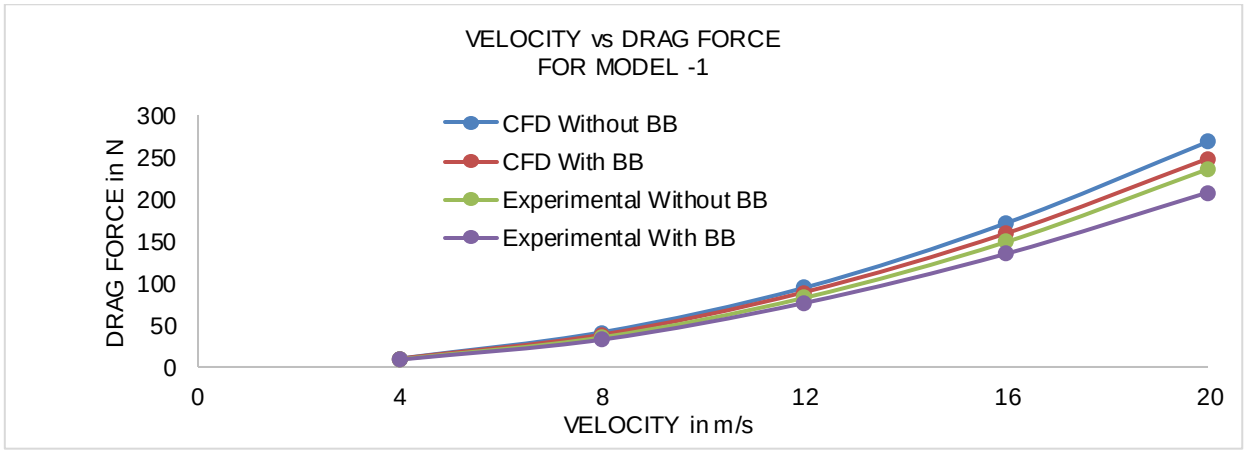

Fig.11 Velocity Vs Drag Force

3.5.Co-efficient of Drag Comparison(Cd)

It is clearly evident from the (Fig.12) graphical representations that the value of Cd decreases due to the addition of base-bleed setup. This can be attributed due to the avoidance of flow separation with the help of base-bleed attachment. For varying velocities Cd will be considerably lesser compared with without base-bleed attachment. Hence, it is observed that base-bleed attachment will be useful at lower velocity to reduce drag co-efficient. Finally, from the above graphical representations it clearly shows that the base-bleed attachment will reduces the drag forces acting on car model on various velocities.

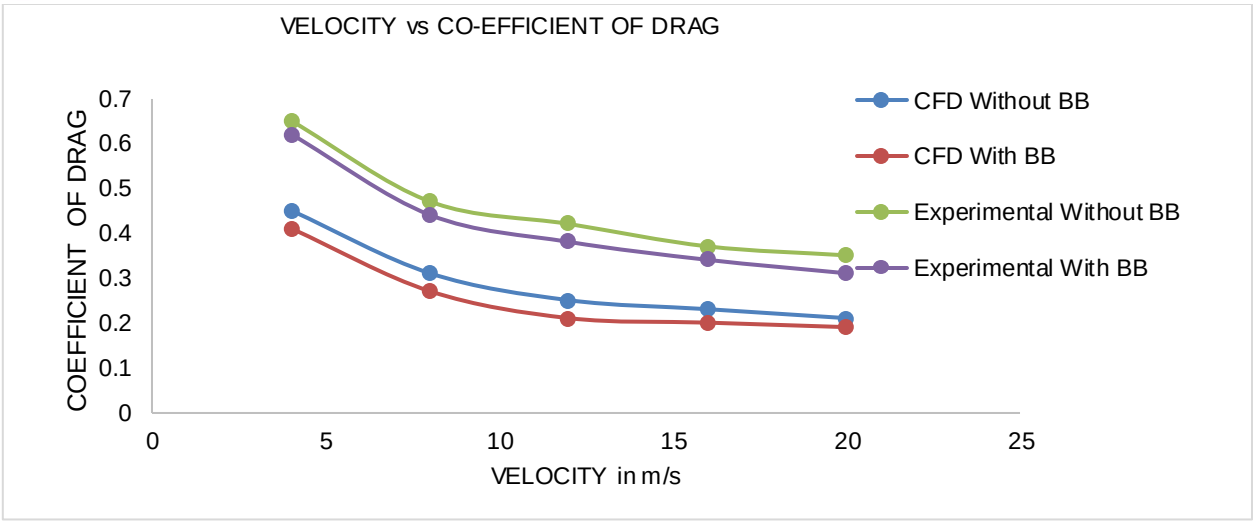

Fig.12 Velocity Vs Drag Force

3.6.Lift force Comparison

It is clearly evident from the (Fig.13) that the value of drag force decreases due to the addition of base-bleed setup. This can be attributed due to the escaping of air flow with the help of base-bleed attachment. For varying velocities Fd will be considerably lesser compared to without base bleed attachment. Even in high velocity also the drag co-efficient will be lesser compared to without base-bleed attachment. Hence, it is observed that base-bleed attachment will be useful at lower velocity to reduce drag force.

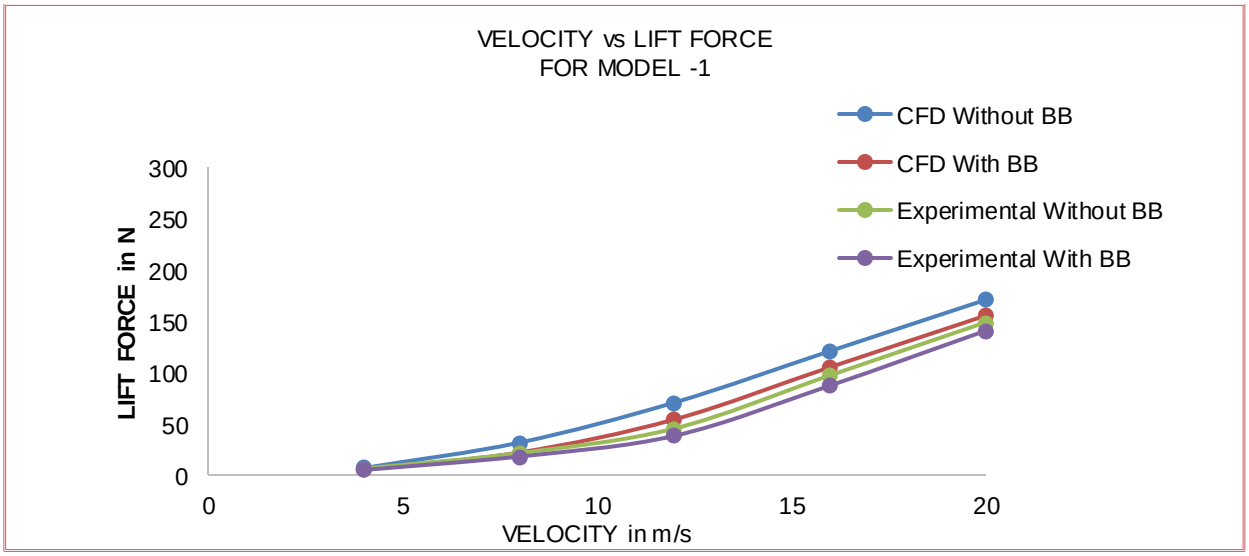

Fig.13 Velocity Vs Drag Force

3.7.Co-efficient of Lift Comparison(Cl)

It is clearly evident from the (Fig.14) graphical representations that the value of Cd decreases due to the addition of base-bleed setup. This can be attributed due to the avoidance of flow separation with the help of base-bleed attachment. For varying velocities Cd will be considerably lesser compared with without base-bleed attachment. Hence, it is observed that base-bleed attachment will be useful at lower velocity to reduce drag co-efficient. Finally, from the above graphical representations it clearly shows that the base-bleed attachment will reduces the drag forces acting on car model on various velocities.

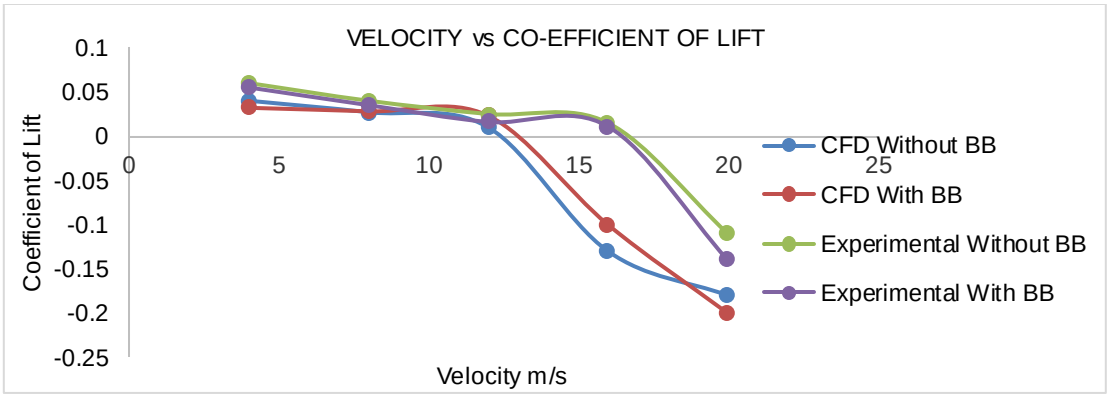

Fig.14 Velocity Vs Coefficient of Lift

3.8. Correlation between the drag coefficient and the Reynolds number

From the (Fig.15) graph shows the drag co-efficient Vs Reynolds's number its shows that when Reynolds number increases the drag co-efficient value will decreases. The drag coefficient Cd converges with increasing Reynolds numbers towards the value Cd=0.20 (with base-bleed attachment) and Cd=0.20 (without base-bleed attachment). The drag coefficient without base bleed is by trend higher than with base bleed, although the difference lessens with growing Reynolds numbers. The boundary layer concept is only valid for large values of the order

$$Re_l = \frac{V_\infty l}{\nu} > 10^4$$

This dimensionless parameter is called the Reynolds number. It is a function of the speed of the vehicle V∞ the kinematic viscosity v of the fluid and a characteristic length of the vehicle, e.g. its total length / as in Fig. 15. The character of viscous flow around a body depends only on the body shape and the Reynolds number. For different Reynolds numbers entirely different flows may occur for the same body geometry. Thus the Reynolds number is the dimensionless parameter that characterizes a viscous flow Hucho WH (1998)(8).

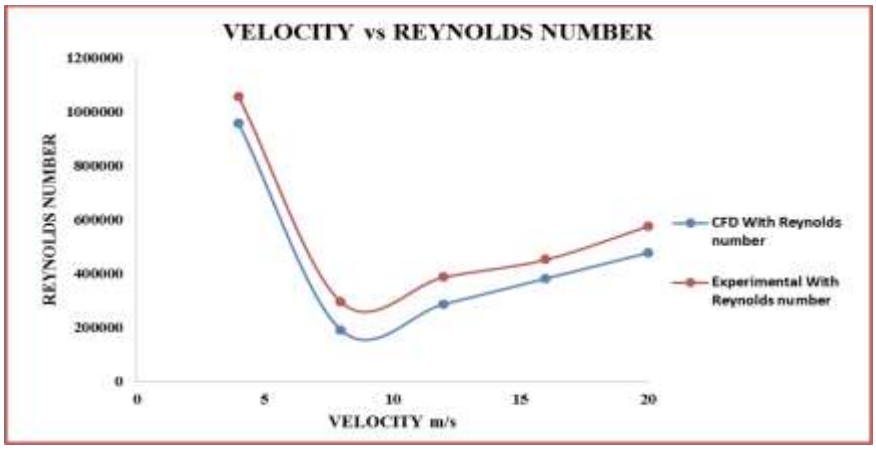

Fig.15 Velocity Vs Reynolds Number

4.CONCLUSIONS

In this paper, the influence of base bleed attached on under body of the realistic hatch back model car was investigated for five free stream velocities (U_∞ = 4, 8, 12, 16, and 20m/s). It has been shown that base bleed can significantly decrease drag when applied to the geometry of a real hatchback model car.

It has also been demonstrated that the influence of the Reynolds number on the drag coefficient lesse ns with augmenting Reynolds numbers and that the investigation of the realistic hatchback model car at the reduced Reynolds number of Re=4.787E+6 is therefore feasible.

The distributions of the pressure coefficient in different velocities were discussed. Again, the realistic hatch back model car geometry shows very similar behavior, while the distribution at the both configurations shows different results.

Ground simulation does not change the pressure distribution at the top of the vehicles. Furthermore, the pressure distribution on different parts of the vehicle surface was evaluated. It has been shown that the base bleed attachment does not influence the distribution of the pressure.

The addition of the device base bleed resulted in a reduction of total drag by 20 percent. Furthermore, the with BB model generates higher base pressure compared to without BB.

This base pressure increase for the with BB configuration is the result of:

1) The initial separation from the trailing edge of the model and it's subsequent reattachment on the rear side which forms a vortex ring and, thereby, a lower pressure area rear side both CFD and experiment. This lower pressure distribution has an adverse effect on the total drag.

2) The flow reattachment on the BB decelerates the outer flow which in turn increases the pressure significantly at the edge of the plates where the flow separates again to form the main recirculation region in the wake. This significant rise in the pressure has a favorable effect on the total drag.

3) The cavity effect for the with BB model. The favorable pressure increases in 2 and 3 outweigh the adverse pressure effect of 1 with a favorable net pressure increase. The stabilization of the near wake due to the device is documented by suppression of the base pressure fluctuation spectral peak at St ~ 0.07 and reduced turbulence level in the wake.

Finally, both experiment and simulation suggest that the drag reduction device strongly influence the underbody flow. The device causes the mean streamlines close to the ground to turn upward more rapidly, and increase the flow velocity in this region. In summary, based on our measurements and the CFD simulations the following conclusions can be drawn.

The mean pressure results show a significant increase in the base pressure when the drag reduction device is in place. The results show a reduction of the turbulence intensity as well as a rapid upward deflection of the underbody flow due to the add-on device compared to the baseline configuration. Finally the reduction of drag implies the fuel economy will be reuced.

Nomenclature

Cd	: Drag Coefficient
Cl	: Lift Coefficient
R	: Reynolds Number
F_D	: Drag Force
F_L	: Lift Force
BB	: Base Bleed

ACKNOWLEDGMENTS

Our thanks to the experts who have contributed towards development of this research work.

REFERENCES

1. Ahmed SR, Ramm R, Faltin G (1984) Some salient features of thetime-averaged ground vehicle wake. SAE paper 840300, pp 1–30
2. Aachenbach E.; 1972; Experiments on the flow past spheres at very high Reynolds numbers; Fluid Mech. 62, 209-221
3. Angelina I. Heft, 2012 ;ThomasIndinger and Nikolaus A. Adams TechnischeUniversitätMünchen Introduction of a New Realistic Generic Car Model for Aerodynamic InvestigationsSAE International doi:10.4271/2012-01-0168
4. Cogotti, A., 1983. Aerodynamic characteristics of car wheel.Impact of Aerodynamics on Vehicle Design. International Journal of Vehicle Design 3, 173–196.
5. Chin-Yi Wei, Jeng-Ren Chang; 2002:Wake and base bleed flow downstream of bluff bodies with different geometry;; Experimental Thermal and Fluid Science 26; 39–52
6. G. K. Suryanarayana, Hemming Pauer, G. E. A. Meier; 1993; Bluff-body drag reduction by passive ventilation; Experiments in Fluids 16, 73-81
7. Hucho WH (1998) Aerodynamics of road vehicles.CambridgeUniversity Press, Cambridge
8. Howell, J., Sims-Williams, D., Sprot, A., Hamlin, F. et al., "Bluff Body Drag Reduction with Ventilated Base Cavities," SAE Int. J. Passeng. Cars - Mech. Syst. 5(1):152-160, 2012, doi:10.4271/2012-01-0171.
9. Howell, J., Sheppard, A., and Blakemore, A., "Aerodynamic Drag Reduction for a Simple Bluff Body Using Base Bleed," SAE Technical Paper 2003-01-0995, 2003, doi:10.4271/2003-01-0995
10. Irving Brown, Y., Windsor, S., and Gaylard, A., "The Effect of Base Bleed and Rear Cavities on the Drag of an SUV," SAE Technical Paper 2010-01-0512, 2010, doi:10.4271/2010-01-0512.155–164
11. Lamond, Andrew and Kennedy, Johnathan J. and Stickland, M.T. (2009) An investigation into unsteady base bleed for drag reduction in bluff two-box SUVs. In: 4th EuropeanAutomotive Simulation Conference, EASC 2009, 6-7 July 2009, Munich, Germany